

PE/ORG-MMT NANOCOMPOSITES Non-isothermal crystallization kinetics

W. Xu^{1,2*}, H. Zhai¹, H. Guo¹, N. Whitely² and W.-P. Pan²

¹Department of Polymer Science and Engineering, Hefei University of Technology, Hefei, 230009 Anhui, China

²Department of Chemistry, Materials Characterization Center, Western Kentucky, Bowling Green, KY, 42101, USA

Abstract

The non-isothermal crystallization kinetics of polyethylene (PE), PE/organic-montmorillonite (Org-MMT) composites were investigated by differential scanning calorimetry (DSC) with various cooling rates. The Avrami analysis modified by Jeziorny and a method developed by Mo were employed to describe the non-isothermal crystallization process of these samples very well. The difference in the exponent n between PE and PE/Org-MMT nanocomposites, indicated that non-isothermal kinetic crystallization corresponded to tridimensional growth with heterogeneous nucleation. The values of half-time, Z_c and $F(T)$ showed that the crystallization rate increased with the increasing of cooling rates for PE and PE/Org-MMT composites, but the crystallization rate of PE/Org-MMT composite was faster than that of PE at a given cooling rate. The method developed by Ozawa did not describe the non-isothermal crystallization process of PE very well. Moreover, the method proposed by Kissinger was used to evaluate the activation energy of the mentioned samples. The results showed that the activation energy of PE/Org-MMT was greatly larger than that of PE.

Keywords: montmorillonite, nanocomposite, non-isothermal crystallization kinetics, polyethylene

Introduction

Polymer/clay nanocomposites are a class of hybrid materials composed of an organic polymer matrix in which inorganic particles with nanoscale dimension are embodied [1–4]. At this scale, the inorganic fillers dramatically improve the properties of polymer even with a small loading. The nanocomposites exhibit improved modulus, lower thermal expansion coefficient and gas permeability, higher swelling resistance and enhanced ionic conductivity compared with the pristine polymers presumably due to the nanoscale structure of the hybrids and the synergism between the polymer and the silicate [5, 6]. Since the nylon/clay nanocomposites with excellent mechanic properties were developed by the Toyota group, much attention has been devoted to polymer/clay nanocomposites [7–9].

* Author for correspondence: E-mail: xwb105105@sina.com

The most commonly used clay is montmorillonite (MMT), which belongs to the general family of 2:1 layered silicates. Their structures consist of two fused silica tetrahedral sheets sandwiching an edge-shared octahedral sheet of either aluminum or magnesium hydroxide. The silicate layers are coupled through relatively weak dipolar and van der Waals forces. The Na^+ or Ca^{2+} residing in the interlayers can be replaced by organic cations such as alkylammonium ions via an ion-exchange reaction to render the hydrophilic-layered silicate organophilic. In most cases, the synthesis of polymer/MMT nanocomposites was reported via either an intercalated polymerization process or a direct melt intercalation. The direct melt intercalation process was the more promising of the two methods because this process does not require any solvents; therefore, it is easily applied in industry [10].

Polyethylene is one of the most widely used polyolefin polymers. Since it does not include any polar groups in its backbone, it is not thought that homogeneous dispersion of clay layers in PE would be realized. Alexandre and coworkers reported the preparation of polyethylene-layered silicate nanocomposites by the polymerization-filling technique [11]. Shin *et al.* used bifunctional organic modifiers to prepare PE/clay hybrid nanocomposites by in situ polymerization [12]. Zhang *et al.* acquired low-density polyethylene (LDPE)-clay nanocomposites with good flammability properties via melt mixing in a Brabender mixer [13]. The results reported concerning to polypropylene-clay hybrid preparation show that chemical modification of these resins, in particular the grafting of pendant anhydride groups, has been proved as a useful way to overcome problems associated with poor phase adhesion in polyolefin/clay systems [10, 14–15]. Therefore, Wang *et al.* prepared linear low-density polyethylene (LLDPE-MAH)/clay nanocomposites by grafting polar monomer maleic anhydride to the backbone [16–18]. Gopakumar also gained PE/clay nanocomposites by direct-melt intercalation and had an investigation of its non-isothermal crystallization kinetics [19].

For the polymer crystallization, generally, studies of crystallization process are limited to isothermal conditions, the theoretical analysis is easy to handle, and problems associated with cooling rates and thermal gradients within specimens are avoided. The isothermal crystallization process of polymers, such as polyoxymethylene (POM) [20], syndiotactic polypropylenes [21], polypropylene and maleic anhydride grafted polypropylene [22] have been studied. In practice, however, the crystallization in a continuously changing thermal environment is of great interest, given that industrial process, generally proceed under non-isothermal conditions. Therefore, more and more attention has being attached to the study of non-isothermal crystallization process for polymers [23–27].

Polyethylene (PE) is a semicrystalline polymer. The final properties of composites based on PE in an engineering application are critically dependent on the extent of crystallinity and the nature of crystalline morphology of PE, which in turn depend on the processing conditions. Thus, it is necessary to understand the relationship between processing conditions and the development, nature, and degree of crystallinity the composites based on PE.

In our previous work, we successfully prepared PE/Org-MMT nanocomposites via melt-direct intercalation [28]. In this paper, several non-isothermal crystallization kinetic equations were used to study the crystallization characteristics of PE/Org-

MMT. Dynamic DSC curves supplied the necessary data. By using an evaluation method proposed by Kissinger, activation energies were also calculated for the crystallization of PE/Org-MMT.

Experimental

Non-isothermal DSC analysis

A TA instruments DSC 2920 was used for measuring non-isothermal crystallization kinetics in the cooling mode from the molten state (melt-crystallization). The temperature and energy readings were calibrated with indium at each cooling rate employed in the measurements. All measurements were carried out in nitrogen atmosphere. The raw samples used here were pure HDPE, PE/Org-MMT (99/1), PE/Org-MMT (97/3), PE/Org-MMT (95/5), respectively, and they were prepared by mould process described in previous paper [28]. For non-isothermal melt-crystallization, the raw sample was heated to 150°C held for 5 min in the cell to eliminate previous thermal history. The samples were cooled at constant rates of 1, 2, 5 and 10 K min⁻¹ respectively. The exothermic crystallization peak was then recorded as a function of temperature.

Results and discussion

Crystallization behavior of PE and PE/Org-MMT

The crystallization exotherms of HDPE, PE/Org-MMT nanocomposite at various cooling rates are presented in Fig. 1. From these curves, some useful parameters, such as the peak temperature (T_p) as a function of crystallization temperature can be

Table 1 Non-isothermal crystallization kinetic parameters for sample

Sample	ϕ /K min ⁻¹	n	Z_c	$t_{1/2}$ /min	T_p /°C
PE	1	3.37	0.044	2.44	121.62
	2	3.41	0.416	1.41	120.68
	5	3.65	1.193	0.74	119.15
	10	3.88	1.315	0.49	117.44
PE/Org-MMT=99/1	1	5.78	0.007	2.33	122.50
	2	4.87	0.641	1.21	121.78
	5	5.67	2.184	0.66	120.60
	10	5.08	1.685	0.44	119.29
PE/Org-MMT=97/3	1	6.93	0.005	2.36	122.57
	2	5.47	0.423	1.39	121.82
	5	5.43	2.266	0.62	120.80
	10	4.97	1.773	0.43	119.63
PE/Org-MMT=95/5	1	7.19	0.003	1.76	122.74
	2	7.00	0.246	1.19	121.91
	5	4.95	1.646	0.63	120.66
	10	5.37	1.641	0.42	119.21

obtained for describing the non-isothermal crystallization behavior of HDPE, PE/Org-MMT. It is clearly seen from Fig. 1 that T_p shifts, as expected, to lower temperature with increasing cooling rate for pure PE and PE/Org-MMT. This can be explained that slower time periods will affect the polymer's crystallization as increasing cooling rate, therefore requiring higher undercooling to initiate crystallization, and the motion of PE molecules cannot follow the cooling temperature when the specimens are cooled fast. Although the difference in T_p is not remarkable enough, just because of small difference of scanning rate, 1, 2, 5, 10 K min⁻¹. Furthermore, for a given cooling rate, T_p of PE/Org-MMT composites is higher than that of pure PE as shown in Table 1. This can be explained as particles of Org-MMT having a heterogeneous nucleation effect on PE macromolecule segments. In the molten state, PE macromolecule segments can be easily physically attached to the surface of particle of Org-MMT, which leads to the crystallization of PE molecules in higher crystallization temperature. Moreover, the difference of T_p between PE/Org-MMT with different content of Org-MMT indicates heterogeneous nucleus effects of Org-MMT.

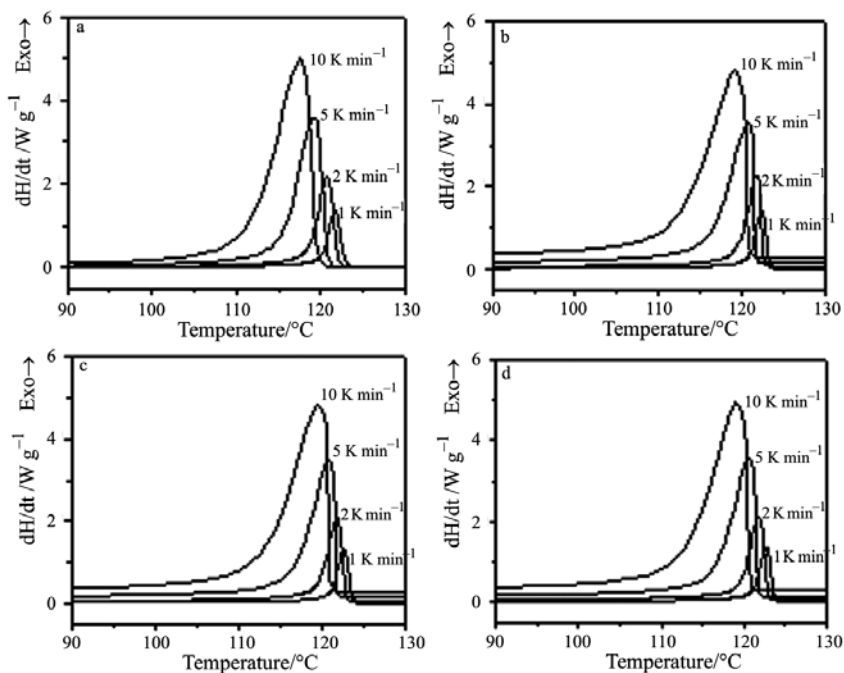


Fig. 1 DSC patterns for PE and PE/Org-MMT during non-isothermal crystallization process. PE/Org-MMT: a – 100/0, b – 99/1, c – 97/3, d – 95/5

Non-isothermal crystallization kinetics of PE and PE/Org-MMT

The relative degree of crystallinity, X_t , as a function of crystallization temperature T is defined as

$$X_t = \frac{\int_{T_0}^T \frac{dHc}{dT} dT}{\int_{T_0}^{T_\infty} \frac{dHc}{dT} dT} \quad (1)$$

where T_0 and T_∞ represent the onset and end of crystallization temperatures, respectively.

Figure 2 shows the development of relative degree of crystallinity as a function of temperature for PE and PE/Org-MMT nanocomposites at various cooling rates. It can be seen that all these curves have the same sigmoidal shape, implying that only the lag effect of cooling rate on crystallization is observed. Using the following equation, $t = (T_0 - T)/\phi$ (T is the temperature at crystallization time t , and ϕ is the cooling rate), the horizontal temperature axis in Fig. 2 could be transformed into a time scale (Fig. 3). It can be seen that the higher the cooling rate is, the shorter the time for completing crystallization is. The half-time of non-isothermal crystallization $t_{1/2}$ could be obtained from Fig. 3 for PE and PE/Org-MMT nanocomposites, and the results are listed in Table 1. It can be seen that, as expected, the value of $t_{1/2}$ decreases with the increasing of cooling rates for PE and PE/Org-MMT nanocomposites. Moreover, at a

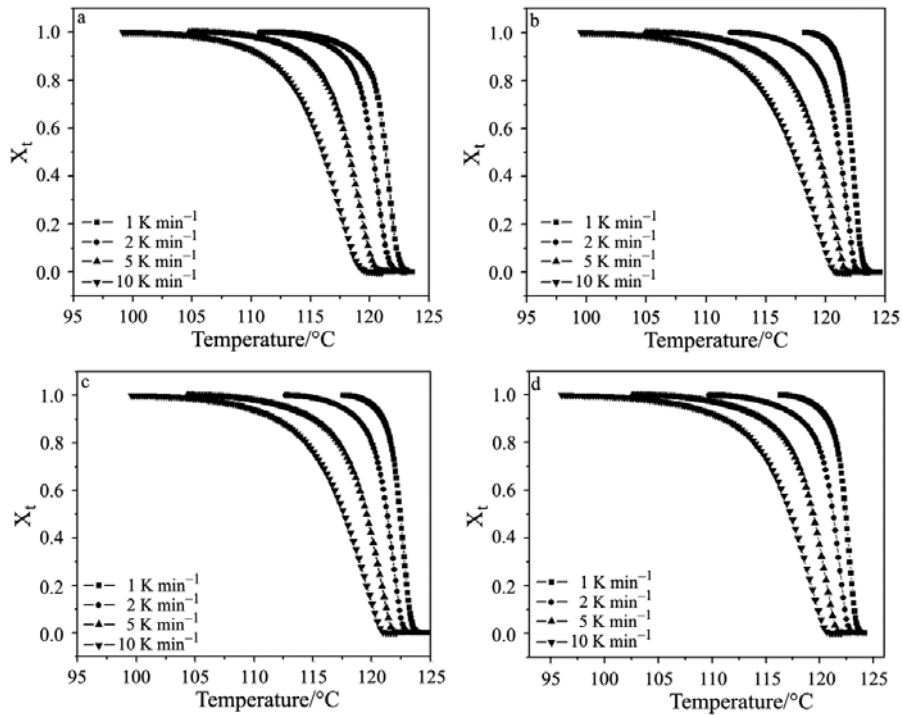


Fig. 2 Patterns of X_t vs. T for nanocomposite during non-isothermal crystallization process.
PE/Org-MMT: a – 100/0, b – 99/1, c – 97/3, d – 95/5

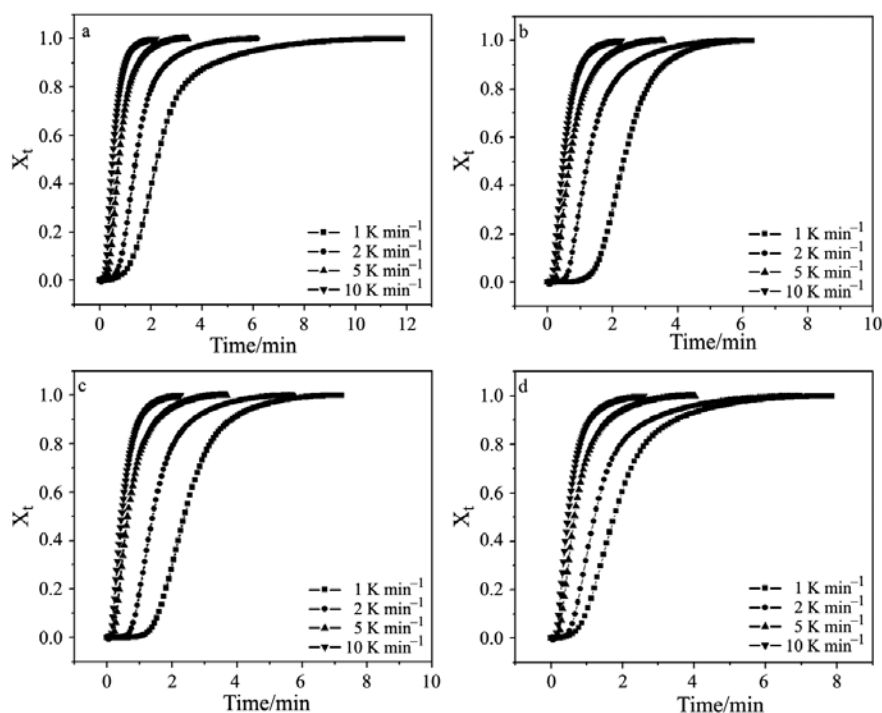


Fig. 3 Plots of X_t vs. t for nanocomposite during non-isothermal crystallization process. PE/Org-MMT: a – 100/0, b – 99/1, c – 97/3, d – 95/5

given cooling rate, the values of $t_{1/2}$ for PE/Org-MMT are lower than that for PE, signifying that the addition of Org-MMT can accelerate the overall crystallization process. The approach adopted here was Avrami equation [29],

$$1 - X_t = \exp(-Z_t t^n) \quad (2)$$

where the exponent n is a mechanism constant depending on the type of nucleation and growth process parameters, and Z_t is a composite rate constant involving both nucleation and growth rate parameters. Using Eq. (2) in double-logarithmic form,

$$\ln(-\ln(1 - X_t)) = \ln Z_t + n \ln t \quad (3)$$

plotting $\ln(-\ln(1 - X_t))$ vs. $\ln t$ for each cooling rate, yields a straight line with the data at low degrees of crystallinity in the linear regression only (Fig. 4), thus two adjustable parameters, Z_t and n , can be estimated. It should be taken into account that in non-isothermal crystallization Z_t and n do not have the same physical significance as in the isothermal crystallization due to the fact that under non-isothermal crystallization the temperature changes constantly. This affects the rates of both nuclei formation and spherulite growth since they are temperature dependent. In this case, Z_t and n are two adjustable parameters only to be fit to the data. Equation (2) can further provide insight into the kinetics of non-isothermal crystallization.

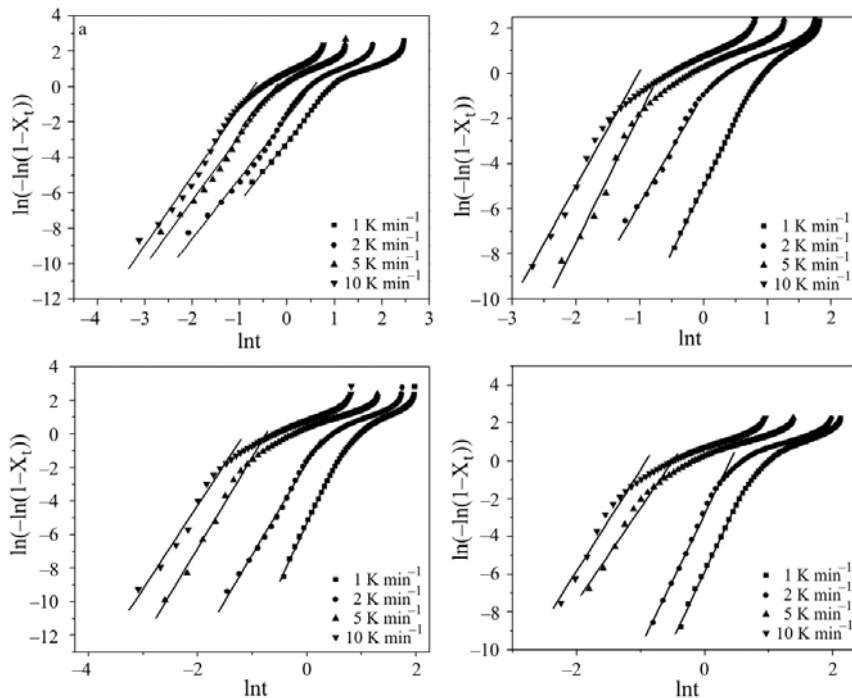


Fig. 4 Plots of $\ln(-\ln(1-X_t))$ vs. $\ln t$ for nanocomposite during non-isothermal crystallization process. PE/Org-MMT: a – 100/0, b – 99/1, c – 97/3, d – 95/5

Considering the non-isothermal character of the process investigated, the final form of the parameter characterizing the kinetics of non-isothermal crystallization was given by Jeziorny [26].

$$\ln Z_c = \ln Z_t / \phi \quad (4)$$

The results obtained from Avrami plots and Jeziorny methods are listed in Table 1. The exponent n of PE varied from 3.3 to 3.8, and from 4.8 to 7.2 for PE/Org-MMT. Although the exponent n in non-isothermal crystallization displayed a wide range of values and was more scattered than those obtained from isothermal crystallization [30], it is interesting that the exponent n for PE/Org-MMT was larger than that for PE at every cooling rate, indicating that non-isothermal crystallization of PE/Org-MMT corresponds to tridimensional growth with heterogeneous nucleation, and the organic-montmorillonite acted as a nucleating agent in PE matrix. For both PE and PE/Org-MMT composites, as expected, the value of Z_c increases with the increasing of cooling rates.

Assuming that non-isothermal crystallization process may be composed of infinitesimally small isothermal crystallization steps, Ozawa [27] extended the Avrami equation to the non-isothermal case as following:

$$1 - X_t = \exp(-K(T)/\phi^m) \quad (5)$$

where $K(T)$ is the function of cooling rate, ϕ the cooling rate and m is the Ozawa exponent depending on the dimension of the crystal growth. Taking the double-logarithmic form:

$$\ln(-\ln(1-X_t)) = \ln K(T) - m \ln \phi \quad (6)$$

and plotting $\ln(-\ln(1-X_t))$ vs. $\ln \phi$ at a given temperature, a straight line should be obtained if the Ozawa method is valid. Thus $K(T)$ and m can be estimated from the intercept and slope, respectively. The results based on Ozawa method are shown in Fig. 5. It is clearly seen that the curves in the plots of $\ln(-\ln(1-X_t))$ vs. $\ln \phi$ for PE and PE/Org-MMT did not exhibit a linear relationship. The reason is at a given temperature the crystallization processes with different cooling rates are at different stages, i.e., lower cooling rate processes are toward the end of the crystallization process, whereas at the higher cooling rate, the crystallization process is at an early stage. That is, the addition of Org-MMT magnified the influence of cooling rate on the crystallization process.

A method developed by Mo [31] was employed to describe the non-isothermal crystallization in order to make comparison. For the non-isothermal crystallization process, physical variables relating to the process are relative degree of crystallinity,

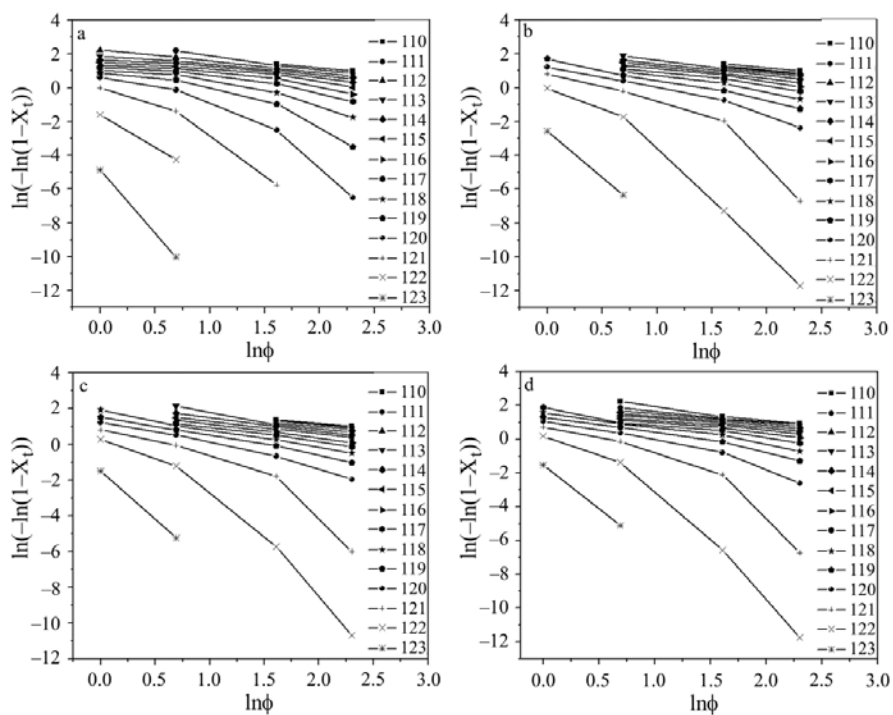


Fig. 5 Plots of $\ln(-\ln(1-X_t))$ vs. $\ln \phi$ for PP and nanocomposite during non-isothermal crystallization process. PE/Org-MMT: a – 100/0, b – 99/1, c – 97/3, d – 95/5

X_t , cooling rate ϕ , and crystallization temperature T . Both Ozawa and Avrami equations give their relationship as following:

$$\ln Z_t + n \ln t = \ln K(T) - m \ln \phi \quad (7)$$

by rearrangement at a given crystallinity X_t

$$\ln \phi = \ln F(T) - a \ln t \quad (8)$$

where $F(T) = [K(T)/Z_t]^{1/m}$ refers to the value of the cooling rate, which must be chosen within unit crystallization time when the measured system amounts to a certain degree of crystallinity, $a = n/m$, the ratio of Avrami exponent n to Ozawa exponent m . According to Eq. (8), at a given degree of crystallinity, plotting $\ln \phi$ vs. $\ln t$ (Fig. 6) yields a linear relationship. The kinetic parameter $F(T)$ and a are determined from the intercept and slope of the lines and are listed in Table 2 for PE and PE/Org-MMT. It can be seen from Table 2 that the value of a for PE varies from 1.41 to 1.57, from 1.10 to 1.65 for PE/Org-MMT nanocomposites, and that $F(T)$ systematically increases with increasing of relative degree of crystallinity. It is also obvious that for a certain relative degree of crystallinity, $F(T)$ for PE/Org-MMT is smaller than that for PE, that is, amounting to same relative degree of crystallinity, PE/Org-MMT requires smaller cooling rates, which indicate that PE/Org-MMT crystallizes at a quicker rate than PE. The conclu-

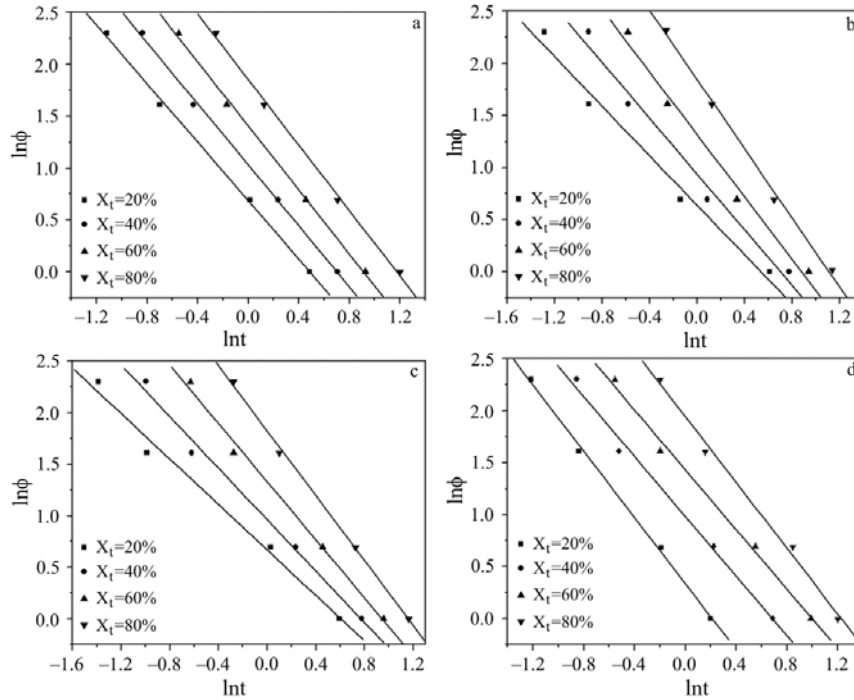


Fig. 6 Plots of $\ln \phi$ vs. $\ln t$ for nanocomposite during non-isothermal crystallization process. PE/Org-MMT: a – 100/0, b – 99/1, c – 97/3, d – 95/5

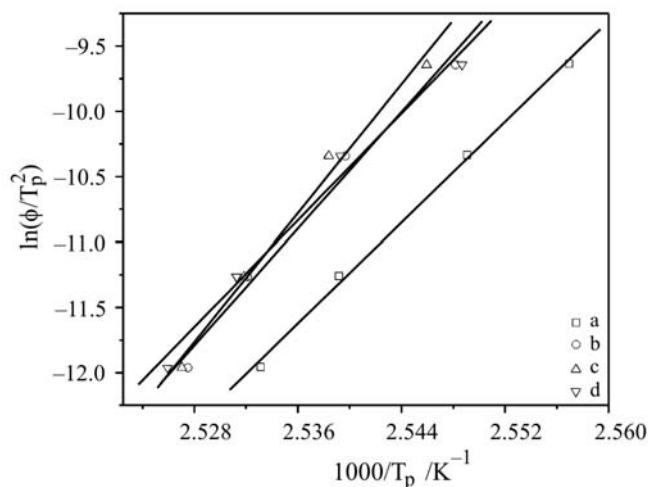


Fig. 7 Plotting of $\ln(\phi/T_p^2)$ vs. $1/T_p$ for PP and composites during non-isothermal crystallization process. PE/Org-MMT: a – 100/0, b – 99/1, c – 97/3, d – 95/5

Table 2 Non-isothermal crystallization kinetic parameters for sample at different relative degree of crystallinity

Sample	$X_t/\%$	a	$F(T)$	$\Delta E/\text{kJ mol}^{-1}$
PE	20	1.41	1.98	96.54
	40	1.47	2.81	
	60	1.54	4.08	
	80	1.57	6.41	
PE/Org-MMT=99/1	20	1.18	1.88	111.59
	40	1.33	2.57	
	60	1.49	3.73	
	80	1.65	6.67	
PE/Org-MMT=97/3	20	1.10	1.94	123.28
	40	1.25	2.62	
	60	1.41	3.80	
	80	1.57	6.22	
PE/Org-MMT=95/5	20	1.59	1.39	102.07
	40	1.44	2.68	
	60	1.44	4.20	
	80	1.58	7.02	

sion agrees with the one drawn from Avrami analysis. Obviously this approach is successful in describing the non-isothermal process of PE and PE/Org-MMT composites as PEEK [31], PHB–PVAc blends [32] and POM/Org-MMT nanocomposite [7].

In addition, the method often used for evaluation of activation energy at various cooling rates based on Eq. (9) was proposed by Kissinger [33]

$$\frac{d[\ln(\phi/T_p^2)]}{d(1/T_p)} = -\frac{\Delta E}{R} \quad (9)$$

where R is the universal gas constant, ΔE is the activation energy of crystallization. Having plotted $\ln(\phi/T_p^2)$ vs. $1/T_p$ (Fig. 7), the activation energies of non-isothermal melt crystallization of PE and PE/Org-MMT composites were determined and are listed in Table 2. As can be seen from Table 2, the value of ΔE for PE/Org-MMT is greatly larger than that of PE, because the Org-MMT particles increase the viscosity of PE, which prevent PE macromolecule segments from rearranging, as a result, the activation energy increases.

Conclusions

The PE/Org-MMT nanocomposites were prepared successfully via melt intercalation, and a TA instruments DSC 2920 was used to investigate the crystallization behavior of PE and PE/Org-MMT nanocomposites from the molten state. It was found that the Avrami analysis modified by Jeziorny and a method developed by Mo were successfully in describing the non-isothermal crystallization process of PE and PE/Org-MMT nanocomposites. The difference in the exponent n between PE and PE/Org-MMT nanocomposite, indicates that non-isothermal kinetic crystallization corresponded to tridimensional growth with heterogeneous nucleation. The half-time $t_{1/2}$, Z_c and $F(T)$ showed that the crystallization rate of PE and PE/Org-MMT nanocomposites increased with increasing of cooling rates, and that the crystallization rate of PE/Org-MMT nanocomposites was faster than that of PE at a given cooling rate. The Ozawa analysis did not offer an adequate description of the non-isothermal crystallization of PE and PE/Org-MMT. The activation energy of PE/Org-MMT was greatly larger than that of PE due to the increased viscosity.

* * *

The authors gratefully acknowledge the financial support (Grant Number: 01402012) from Committee of Science and Technology of Anhui Province, China.

References

- 1 P. B. Messersmith and E. P. Giannelis, *J. Polym. Sci. Part A: Polym. Chem.*, 33 (1995) 1047.
- 2 A. Usuki, T. Kawasumi, M. Kojima, Y. Fukushima and A. Okada, *J. Mater. Res.*, 8 (1993) 1179.
- 3 Y. Kojima, A. Usuki, M. Kawasumi, Y. Fukushima, A. Okada and T. Kurauchi, *J. Mater. Res.*, 8 (1993) 1185.
- 4 K. Yano, A. Usuki, A. Okada, T. Kurauchi and O. Kamigato, *J. Polym. Sci. Part A: Polym. Chem.*, 31 (1993) 2493.
- 5 E. P. Giannelis, *Adv. Mater.*, 8 (1996) 29.
- 6 Z. Wang and T. J. Piamavaia, *Chem. Mater.*, 10 (1998) 3769.
- 7 W. B. Xu, M. I. Ge and P. S. He, *J. Appl. Polym. Sci.*, 82 (2001) 2281.
- 8 W. B. Xu, M. L. Ge and P. S. He, *China Plastic*, 14 (2000) 28.

- 9 W. B. Xu, S. P. Bao and P. S. He, *J. Polym. Sci.*, 84 (2002) 842.
- 10 P. Hoai Nam, P. Maiti, M. Okamoto, T. Kotaka, N. Hasegawa and A. Usuki, *Polymer*, 42 (2001) 9633.
- 11 M. Alexandre, P. Dubois, T. Sun, J. M. Garces and R. Jerome, *Polymer*, 42 (2002) 2123.
- 12 A. S. Y. Shin, L. C. Simon, J. B. P. Soares and G. Scholz, *Polymer*, 44 (2003) 5317.
- 13 J. G. Zhang and C. A. Wilkie, *Polym. Degrad. Stab.*, 80 (2003) 163.
- 14 M. Kato, A. Usuki and A. Okada, *J. Appl. Polym. Sci.*, 66 (1997) 1781.
- 15 M. Kawasumi, N. Hasegawa, M. Kato, A. Usuki and A. Okada, *Macromolecules*, 30 (1997) 6333.
- 16 K. H. Wang, M. H. Choi, C. M. Koo, Y. S. Choi and I. J. Chung, *Polymer*, 42 (2001) 9819.
- 17 C. M. Koo, H. T. Ham, S. O. Kim, K. H. Wang and I. J. Chung, *Macromolecules*, 35 (2002) 5116.
- 18 K. H. Wang, I. J. Chung, M. O. Jang, J. K. Keum and H. H. Song, *Macromolecules*, 35 (2002) 5529.
- 19 T. G. Gopakumar, J. A. Lee and M. Kontopoulou, *Parent JS Polymer*, 43 (2002) 5483.
- 20 W. B. Xu and P. S. He, *J. Application Poly. Sci.*, 80 (2001) 304.
- 21 P. Supaphol and J. E. Spruiell, *Polymer*, 41 (2000) 1205.
- 22 Y. Seo, J. Kim, K. U. Kim and Y. C. Kim, *Polymer*, 41 (2000) 2639.
- 23 W. B. Xu, M. L. Ge and P. S. He, *J. Polym. Sci. Part B: Polym. Phys.*, 40 (2002) 408.
- 24 L. Markus, *Polym. Eng. Sci.*, 38 (1998) 610.
- 25 K. Nakamura, T. Watanabe, K. Katayama and T. Amano, *J. Appl. Polym. Sci.*, 16 (1972) 1077.
- 26 A. Jeziorny, *Polymer*, 19 (1978) 1142.
- 27 T. Ozawa, *Polymer*, 12 (1971) 150.
- 28 W. B. Xu, H. P. Zhar and H. Y. Guo, *European Polym. J.*, submitted.
- 29 M. J. Avrami, *Chem. Phys.*, 9 (1941) 177.
- 30 S. Srinivas, J. R. Babu, J. S. Riffle and G. L. Wilkes, *Polym. Eng. Sci.*, 37 (1997) 497.
- 31 T. X. Liu, Z. S. Mo, S. E. Wang and H. F. Zhang, *Polym. Eng. Sci.*, 37 (1997) 568.
- 32 Y. Ar, L. Li, Z. S. Mo and Z. L. Peng, *J. Polym. Sci. Part B: Polym. Phys.*, 37 (1999) 443.
- 33 H. E. Kissinger, *J. Res. Nat. Bur. Stand. (US)*, 57 (1956) 217.